Observation of the W-annihilation decay $D_s^+ \to \omega\pi^+$ and evidence for $D_s^+ \to \omega K^+$

M. Ablikim,[1] M. N. Achasov,[10,d] S. Ahmed,[15] M. Albrecht,[4] M. Alekseev,[56a,56c] A. Amoroso,[56a,56c] F. F. An,[1] Q. An,[53,43] Y. Bai,[42] O. Bakina,[27] R. Baldini Ferroli,[23a] Y. Ban,[35] K. Begzsuren,[25] D. W. Bennett,[22] J. V. Bennett,[5] N. Berger,[26] M. Bertani,[23a] D. Bettoni,[24a] F. Bianchi,[56a,56c] E. Boger,[27,b] I. Boyko,[27] R. A. Briere,[5] H. Cai,[58] X. Cai,[1,43] O. Cakir,[46a] A. Calcaterra,[23a] G. F. Cao,[1,47] S. A. Cetin,[46b] J. Chai,[56c] J. F. Chang,[1,43] W. L. Chang,[1,47] G. Chelkov,[27,b,c] G. Chen,[1] H. S. Chen,[1,47] J. C. Chen,[1] M. L. Chen,[1,43] P. L. Chen,[54] S. J. Chen,[33] Y. B. Chen,[1,43] W. Cheng,[56c] G. Cibinetto,[24a] F. Cossio,[56c] H. L. Dai,[1,43] J. P. Dai,[38,h] A. Dbeyssi,[15] D. Dedovich,[27] Z. Y. Deng,[1] A. Denig,[26] I. Denysenko,[27] M. Destefanis,[56a,56c] F. De Mori,[56a,56c] Y. Ding,[31] C. Dong,[34] J. Dong,[1,43] L. Y. Dong,[1,47] M. Y. Dong,[1,43,47] Z. L. Dou,[33] S. X. Du,[61] P. F. Duan,[1] J. Z. Fan,[45] J. Fang,[1,43] S. S. Fang,[1,47] Y. Fang,[1] R. Farinelli,[24a,24b] L. Fava,[56b,56c] S. Fegan,[26] F. Feldbauer,[4] G. Felici,[23a] C. Q. Feng,[53,43] M. Fritsch,[4] C. D. Fu,[1] Y. Fu,[1] Q. Gao,[1] X. L. Gao,[53,43] Y. Gao,[45] Y. G. Gao,[6] Z. Gao,[53,43] B. Garillon,[26] I. Garzia,[24a] A. Gilman,[50] K. Goetzen,[11] L. Gong,[34] W. X. Gong,[1,43] W. Gradl,[26] M. Greco,[56a,56c] L. M. Gu,[33] M. H. Gu,[1,43] S. Gu,[2] Y. T. Gu,[13] A. Q. Guo,[1] L. B. Guo,[32] R. P. Guo,[1,47] Y. P. Guo,[26] A. Guskov,[27] Z. Haddadi,[29] S. Han,[58] X. Q. Hao,[16] F. A. Harris,[48] K. L. He,[1,47] F. H. Heinsius,[4] T. Held,[4] Y. K. Heng,[1,43,47] T. Holtmann,[4] Z. L. Hou,[1] H. M. Hu,[1,47] J. F. Hu,[38,h] T. Hu,[1,43,47] Y. Hu,[1] G. S. Huang,[53,43] J. S. Huang,[16] X. T. Huang,[37] X. Z. Huang,[33] T. Hussain,[55] W. Ikegami Andersson,[57] M. Irshad,[53,43] Q. Ji,[1] Q. P. Ji,[16] X. B. Ji,[1,47] X. L. Ji,[1,43] X. S. Jiang,[1,43,47] X. Y. Jiang,[34] J. B. Jiao,[37] Z. Jiao,[18] D. P. Jin,[1,43,47] S. Jin,[1,47] Y. Jin,[49] T. Johansson,[57] A. Julin,[50] N. Kalantar-Nayestanaki,[29] X. S. Kang,[34] M. Kavatsyuk,[29] B. C. Ke,[1] T. Khan,[53,43] A. Khoukaz,[51] P. Kiese,[26] R. Kiuchi,[1] R. Kliemt,[11] L. Koch,[28] O. B. Kolcu,[46b,f] B. Kopf,[4] M. Kornicer,[48] M. Kuemmel,[4] M. Kuessner,[4] A. Kupsc,[57] M. Kurth,[1] W. Kühn,[28] J. S. Lange,[28] M. Lara,[22] P. Larin,[15] L. Lavezzi,[56c] S. Leiber,[4] H. Leithoff,[26] C. Li,[57] Cheng Li,[53,43] D. M. Li,[61] F. Li,[1,43] F. Y. Li,[35] G. Li,[1] H. B. Li,[1,47] H. J. Li,[1,47] J. C. Li,[1] J. W. Li,[41] Ke Li,[1] Lei Li,[3] P. L. Li,[53,43] P. R. Li,[47,7] Q. Y. Li,[37] T. Li,[37] W. D. Li,[1,47] W. G. Li,[1] X. L. Li,[37] X. N. Li,[1,43] X. Q. Li,[34] Z. B. Li,[44] H. Liang,[53,43] Y. F. Liang,[40] Y. T. Liang,[28] G. R. Liao,[12] L. Z. Liao,[1,47] J. Libby,[21] C. X. Lin,[44] D. X. Lin,[15] B. Liu,[38,h] B. J. Liu,[1] C. X. Liu,[1] D. Liu,[53,43] D. Y. Liu,[38,h] F. H. Liu,[39] Fang Liu,[1] Feng Liu,[6] H. B. Liu,[13] H. L. Liu,[42] H. M. Liu,[1,47] Huanhuan Liu,[1] Huihui Liu,[17] J. B. Liu,[53,43] J. Y. Liu,[1,47] K. Liu,[45] K. Y. Liu,[31] Ke Liu,[6] Q. Liu,[47] S. B. Liu,[53,43] X. Liu,[30] Y. B. Liu,[34] Z. A. Liu,[1,43,47] Zhiqing Liu,[26] Y. F. Long,[35] X. C. Lou,[1,43,47] H. J. Lu,[18] J. D. Lu,[1,47] J. G. Lu,[1,43] Y. Lu,[1] Y. P. Lu,[1,43] C. L. Luo,[32] M. X. Luo,[60] T. Luo,[9,j] X. L. Luo,[1,43] S. Lusso,[56c] X. R. Lyu,[47] F. C. Ma,[31] H. L. Ma,[1] L. L. Ma,[37] M. M. Ma,[1,47] Q. M. Ma,[1] X. N. Ma,[34] X. X. Ma,[1,47] X. Y. Ma,[1,43] Y. M. Ma,[37] F. E. Maas,[15] M. Maggiora,[56a,56c] S. Maldaner,[26] Q. A. Malik,[55] A. Mangoni,[23b] Y. J. Mao,[35] Z. P. Mao,[1] S. Marcello,[56a,56c] Z. X. Meng,[49] J. G. Messchendorp,[29] G. Mezzadri,[24a] J. Min,[1,43] T. J. Min,[1] R. E. Mitchell,[22] X. H. Mo,[1,43,47] Y. J. Mo,[6] C. Morales Morales,[15] G. Morello,[23a] N. Yu. Muchnoi,[10,d] H. Muramatsu,[50] A. Mustafa,[4] S. Nakhoul,[11,g] Y. Nefedov,[27] F. Nerling,[11,g] I. B. Nikolaev,[10,d] Z. Ning,[1,43] S. Nisar,[8,l] S. L. Niu,[1,43] S. L. Olsen,[36,k] Q. Ouyang,[1,43,47] S. Pacetti,[23b] Y. Pan,[53,43] M. Papenbrock,[57] P. Patteri,[23a] M. Pelizaeus,[4] J. Pellegrino,[56a,56c] H. P. Peng,[53,43] K. Peters,[11,g] J. Pettersson,[57] J. L. Ping,[32] R. G. Ping,[1,47] A. Pitka,[4] R. Poling,[50] V. Prasad,[53,43] H. R. Qi,[2] M. Qi,[33] T. Y. Qi,[2] S. Qian,[1,43] C. F. Qiao,[47] N. Qin,[58] X. S. Qin,[4] Z. H. Qin,[1,43] J. F. Qiu,[1] K. H. Rashid,[55,i] K. Ravindran,[21] C. F. Redmer,[26] M. Richter,[4] M. Ripka,[26] A. Rivetti,[56c] M. Rolo,[56c] G. Rong,[1,47] Ch. Rosner,[15] M. Rump,[51] A. Sarantsev,[27,e] M. Savrié,[24b] C. Schnier,[4] K. Schoenning,[57] W. Shan,[19] X. Y. Shan,[53,43] M. Shao,[53,43] C. P. Shen,[2] P. X. Shen,[34] X. Y. Shen,[1,47] H. Y. Sheng,[1] X. Shi,[1,43] J. J. Song,[37] W. M. Song,[37] X. Y. Song,[1] S. Sosio,[56a,56c] C. Sowa,[4] S. Spataro,[56a,56c] G. X. Sun,[1] J. F. Sun,[16] L. Sun,[58] S. S. Sun,[1,47] X. H. Sun,[1] Y. J. Sun,[53,43] Y. K. Sun,[53,43] Y. Z. Sun,[1] Z. J. Sun,[1,43] Z. T. Sun,[22] Y. T. Tan,[53,43] C. J. Tang,[40] G. Y. Tang,[1] X. Tang,[1] I. Tapan,[46c] M. Tiemens,[29] B. Tsednee,[25] I. Uman,[46d] G. S. Varner,[48] B. Wang,[1] B. L. Wang,[47] C. W. Wang,[33] D. Y. Wang,[35] Dan Wang,[47] K. Wang,[1,43] L. L. Wang,[1] L. S. Wang,[1] M. Wang,[37] Meng Wang,[1,47] P. Wang,[1] P. L. Wang,[1] W. P. Wang,[53,43] X. F. Wang,[1] Y. Wang,[53,43] Y. F. Wang,[1,43,47] Y. Q. Wang,[26] Z. Wang,[1,43] Z. G. Wang,[1,43] Z. Y. Wang,[1] Zongyuan Wang,[1,47] T. Weber,[4] D. H. Wei,[12] P. Weidenkaff,[26] S. P. Wen,[1] U. Wiedner,[4] M. Wolke,[57] L. H. Wu,[1] L. J. Wu,[1,47] Z. Wu,[1,43] L. Xia,[53,43] X. Xia,[37] Y. Xia,[20] D. Xiao,[1] Y. J. Xiao,[1,47] Z. J. Xiao,[32] Y. G. Xie,[1,43] Y. H. Xie,[6] X. A. Xiong,[1,47] Q. L. Xiu,[1,43] G. F. Xu,[1] J. J. Xu,[1,47] L. Xu,[1] Q. J. Xu,[14] Q. N. Xu,[47] X. P. Xu,[41] F. Yan,[54] L. Yan,[56a,56c] W. B. Yan,[53,43] W. C. Yan,[2] Y. H. Yan,[20] H. J. Yang,[38,h] H. X. Yang,[1] L. Yang,[58] S. L. Yang,[1,47] Y. H. Yang,[33] Y. X. Yang,[12] Yifan Yang,[1,47] Z. Q. Yang,[20] M. Ye,[1,43] M. H. Ye,[7] J. H. Yin,[1] Z. Y. You,[44] B. X. Yu,[1,43,47] C. X. Yu,[34] J. S. Yu,[20] C. Z. Yuan,[1,47] Y. Yuan,[1] A. Yuncu,[46b,a] A. A. Zafar,[55] A. Zallo,[23a] Y. Zeng,[20] Z. Zeng,[53,43] B. X. Zhang,[1] B. Y. Zhang,[1,43] C. C. Zhang,[1] D. H. Zhang,[1] H. H. Zhang,[44] H. Y. Zhang,[1,43] J. Zhang,[1,47] J. L. Zhang,[59] J. Q. Zhang,[4] J. W. Zhang,[1,43,47] J. Y. Zhang,[1] J. Z. Zhang,[1,47] K. Zhang,[1,47] L. Zhang,[45] S. F. Zhang,[33] T. J. Zhang,[38,h] X. Y. Zhang,[37] Y. Zhang,[53,43] Y. H. Zhang,[1,43] Y. T. Zhang,[53,43] Yang Zhang,[1] Yao Zhang,[1] Yu Zhang,[47] Z. H. Zhang,[6] Z. P. Zhang,[53] Z. Y. Zhang,[58] G. Zhao,[1] J. W. Zhao,[1,43] J. Y. Zhao,[1,47] J. Z. Zhao,[1,43] Lei Zhao,[53,43] Ling Zhao,[1] M. G. Zhao,[34] Q. Zhao,[1] S. J. Zhao,[61] T. C. Zhao,[1] Y. B. Zhao,[1,43] Z. G. Zhao,[53,43] A. Zhemchugov,[27,b] B. Zheng,[54]

J. P. Zheng,[1,43] W. J. Zheng,[37] Y. H. Zheng,[47] B. Zhong,[32] L. Zhou,[1,43] Q. Zhou,[1,47] X. Zhou,[58] X. K. Zhou,[53,43] X. R. Zhou,[53,43] X. Y. Zhou,[1] Xiaoyu Zhou,[20] Xu Zhou,[20] A. N. Zhu,[1,47] J. Zhu,[34] J. Zhu,[44] K. Zhu,[1] K. J. Zhu,[1,43,47] S. Zhu,[1] S. H. Zhu,[52] X. L. Zhu,[45] Y. C. Zhu,[53,43] Y. S. Zhu,[1,47] Z. A. Zhu,[1,47] J. Zhuang,[1,43] B. S. Zou,[1] and J. H. Zou[1]

(BESIII Collaboration)

[1]*Institute of High Energy Physics, Beijing 100049, People's Republic of China*
[2]*Beihang University, Beijing 100191, People's Republic of China*
[3]*Beijing Institute of Petrochemical Technology, Beijing 102617, People's Republic of China*
[4]*Bochum Ruhr-University, D-44780 Bochum, Germany*
[5]*Carnegie Mellon University, Pittsburgh, Pennsylvania 15213, USA*
[6]*Central China Normal University, Wuhan 430079, People's Republic of China*
[7]*China Center of Advanced Science and Technology, Beijing 100190, People's Republic of China*
[8]*COMSATS University Islamabad, Lahore Campus, Defence Road, Off Raiwind Road, 54000 Lahore, Pakistan*
[9]*Fudan University, Shanghai 200443, People's Republic of China*
[10]*G.I. Budker Institute of Nuclear Physics SB RAS (BINP), Novosibirsk 630090, Russia*
[11]*GSI Helmholtzcentre for Heavy Ion Research GmbH, D-64291 Darmstadt, Germany*
[12]*Guangxi Normal University, Guilin 541004, People's Republic of China*
[13]*Guangxi University, Nanning 530004, People's Republic of China*
[14]*Hangzhou Normal University, Hangzhou 310036, People's Republic of China*
[15]*Helmholtz Institute Mainz, Johann-Joachim-Becher-Weg 45, D-55099 Mainz, Germany*
[16]*Henan Normal University, Xinxiang 453007, People's Republic of China*
[17]*Henan University of Science and Technology, Luoyang 471003, People's Republic of China*
[18]*Huangshan College, Huangshan 245000, People's Republic of China*
[19]*Hunan Normal University, Changsha 410081, People's Republic of China*
[20]*Hunan University, Changsha 410082, People's Republic of China*
[21]*Indian Institute of Technology Madras, Chennai 600036, India*
[22]*Indiana University, Bloomington, Indiana 47405, USA*
[23a]*INFN Laboratori Nazionali di Frascati, I-00044 Frascati, Italy*
[23b]*INFN and University of Perugia, I-06100 Perugia, Italy*
[24a]*INFN Sezione di Ferrara, I-44122 Ferrara, Italy*
[24b]*University of Ferrara, I-44122 Ferrara, Italy*
[25]*Institute of Physics and Technology, Peace Ave. 54B, Ulaanbaatar 13330, Mongolia*
[26]*Johannes Gutenberg University of Mainz, Johann-Joachim-Becher-Weg 45, D-55099 Mainz, Germany*
[27]*Joint Institute for Nuclear Research, 141980 Dubna, Moscow region, Russia*
[28]*Justus-Liebig-Universitaet Giessen, II. Physikalisches Institut, Heinrich-Buff-Ring 16, D-35392 Giessen, Germany*
[29]*KVI-CART, University of Groningen, NL-9747 AA Groningen, Netherlands*
[30]*Lanzhou University, Lanzhou 730000, People's Republic of China*
[31]*Liaoning University, Shenyang 110036, People's Republic of China*
[32]*Nanjing Normal University, Nanjing 210023, People's Republic of China*
[33]*Nanjing University, Nanjing 210093, People's Republic of China*
[34]*Nankai University, Tianjin 300071, People's Republic of China*
[35]*Peking University, Beijing 100871, People's Republic of China*
[36]*Seoul National University, Seoul 151-747, Korea*
[37]*Shandong University, Jinan 250100, People's Republic of China*
[38]*Shanghai Jiao Tong University, Shanghai 200240, People's Republic of China*
[39]*Shanxi University, Taiyuan 030006, People's Republic of China*
[40]*Sichuan University, Chengdu 610064, People's Republic of China*
[41]*Soochow University, Suzhou 215006, People's Republic of China*
[42]*Southeast University, Nanjing 211100, People's Republic of China*
[43]*State Key Laboratory of Particle Detection and Electronics, Beijing 100049, Hefei 230026, People's Republic of China*
[44]*Sun Yat-Sen University, Guangzhou 510275, People's Republic of China*
[45]*Tsinghua University, Beijing 100084, People's Republic of China*
[46a]*Ankara University, 06100 Tandogan, Ankara, Turkey*
[46b]*Istanbul Bilgi University, 34060 Eyup, Istanbul, Turkey*
[46c]*Uludag University, 16059 Bursa, Turkey*

[46d]Near East University, Nicosia, North Cyprus, Mersin 10, Turkey
[47]University of Chinese Academy of Sciences, Beijing 100049, People's Republic of China
[48]University of Hawaii, Honolulu, Hawaii 96822, USA
[49]University of Jinan, Jinan 250022, People's Republic of China
[50]University of Minnesota, Minneapolis, Minnesota 55455, USA
[51]University of Muenster, Wilhelm-Klemm-Str. 9, 48149 Muenster, Germany
[52]University of Science and Technology Liaoning, Anshan 114051, People's Republic of China
[53]University of Science and Technology of China, Hefei 230026, People's Republic of China
[54]University of South China, Hengyang 421001, People's Republic of China
[55]University of the Punjab, Lahore-54590, Pakistan
[56a]University of Turin, I-10125 Turin, Italy
[56b]University of Eastern Piedmont, I-15121 Alessandria, Italy
[56c]INFN, I-10125 Turin, Italy
[57]Uppsala University, Box 516, SE-75120 Uppsala, Sweden
[58]Wuhan University, Wuhan 430072, People's Republic of China
[59]Xinyang Normal University, Xinyang 464000, People's Republic of China
[60]Zhejiang University, Hangzhou 310027, People's Republic of China
[61]Zhengzhou University, Zhengzhou 450001, People's Republic of China

(Received 3 November 2018; published 13 May 2019)

We report the observation of W-annihilation decay $D_s^+ \to \omega\pi^+$ and evidence for $D_s^+ \to \omega K^+$ in a data sample corresponding to an integrated luminosity of 3.19 fb^{-1} collected with the BESIII detector at a center-of-mass energy $\sqrt{s} = 4.178$ GeV. We obtain the branching fractions $\mathcal{B}(D_s^+ \to \omega\pi^+) = (1.77 \pm 0.32_{\rm stat} \pm 0.13_{\rm sys}) \times 10^{-3}$ with a significance of 6.7σ and $\mathcal{B}(D_s^+ \to \omega K^+) = (0.87 \pm 0.24_{\rm stat} \pm 0.08_{\rm sys}) \times 10^{-3}$ with a significance of 4.4σ. This measurement provides critical information to determine the nonperturbative W-annihilation amplitudes and shows the potential of searching for CP asymmetry in $D_s^+ \to \omega K^+$.

DOI: 10.1103/PhysRevD.99.091101

[a]Also at Bogazici University, 34342 Istanbul, Turkey.
[b]Also at the Moscow Institute of Physics and Technology, Moscow 141700, Russia.
[c]Also at the Functional Electronics Laboratory, Tomsk State University, Tomsk 634050, Russia.
[d]Also at the Novosibirsk State University, Novosibirsk 630090, Russia.
[e]Also at the NRC "Kurchatov Institute", PNPI, Gatchina 188300, Russia.
[f]Also at Istanbul Arel University, 34295 Istanbul, Turkey.
[g]Also at Goethe University Frankfurt, 60323 Frankfurt am Main, Germany.
[h]Also at Key Laboratory for Particle Physics, Astrophysics and Cosmology, Ministry of Education; Shanghai Key Laboratory for Particle Physics and Cosmology; Institute of Nuclear and Particle Physics, Shanghai 200240, People's Republic of China.
[i]Also at Government College Women University, Sialkot—51310, Punjab, Pakistan.
[j]Also at Key Laboratory of Nuclear Physics and Ion-beam Application (MOE) and Institute of Modern Physics, Fudan University, Shanghai 200443, People's Republic of China.
[k]Currently at: Center for Underground Physics, Institute for Basic Science, Daejeon 34126, Korea.
[l]Also at Harvard University, Department of Physics, Cambridge, Massachusetts 02138, USA.

Within the Standard Model of particle physics, direct CP violation (CPV) in hadronic decays can only be induced in decays that proceed via at least two distinct decay amplitudes with nontrivial strong and weak phase differences [1–3]. In the charm sector, examples for such decays are singly Cabibbo suppressed (SCS) decays including W-annihilation, tree and penguin amplitudes [1–4], for example $D_s^+ \to \omega K^+$ and other VP final state (V and P refer to vector and pseudoscalar mesons, respectively). However, in D decays, the W-annihilation amplitude is shadowed by tree amplitudes and dominated by nonfactorizable long-distance effects induced by final-state interaction. The theoretical calculation of W-annihilation amplitude is unreliable, which results in some ambiguity in predictions of branching fractions (BFs) and CP asymmetry of related decays. Instead, experimental BF measurements of decays that proceed through W-annihilation are used as input in theoretical calculations [2–5]. Therefore, the BF of the Cabibbo favored (CF) decay $D_s^+ \to \omega\pi^+$, which proceeds only via the W-annihilation process [6], provides direct knowledge of the W-annihilation amplitude.

Compared with the SCS decays, the BF of the CF decay is expected to be larger and may be measured with a higher precision, and is thus more useful experimental input in the W-annihilation amplitude determination. Evidence for

$D_s^+ \to \omega\pi^+$ was first reported by CLEO II experiment in 1997, and a ratio $\frac{\Gamma(D_s^+\to\omega\pi^+)}{\Gamma(D_s^+\to\eta\pi^+)} = 0.16 \pm 0.04 \pm 0.03$ was measured based on 4.7 fb^{-1} data taken at the $\Upsilon(4S)$ peak [6]. Later in 2009, using a data sample corresponding to an integrated luminosity of 0.586 fb^{-1} taken at a center-of-mass energy $\sqrt{s} = 4.170$ GeV, the CLEO-c experiment observed 6.0 ± 2.4 signal events and measured the absolute BF of $D_s^+ \to \omega\pi^+$ to be $(2.1 \pm 0.9 \pm 0.1) \times 10^{-3}$ [7].

With the experimental measurements for $D \to VP$ decays given in Particle Data Group (PDG) [8], theorists predicted the BF and CP asymmetry for $D_s^+ \to \omega K^+$ [3], which implies the potential of searching for CPV in this decay. When the $\rho - \omega$ mixing is considered, the BF and CP asymmetry are predicted to be 0.07×10^{-3} and -2.3×10^{-3} [3], respectively, where the asymmetry is among the largest CP asymmetries in D decays. However, when $\rho - \omega$ mixing is neglected in this decay, the corresponding values are predicted to be 0.6×10^{-3} and -0.6×10^{-3} [3], respectively. The search for $D_s^+ \to \omega K^+$ will test whether $D_s^+ \to \omega K^+$ is a good decay to search for CPV in charm decays.

In this paper, we report measurements of the absolute BFs of the hadronic decays $D_s^+ \to \omega\pi^+$ and $D_s^+ \to \omega K^+$ (charge conjugation is implied throughout this paper). At the center-of-mass energy of $\sqrt{s} = 4.178$ GeV, the D_s^+ meson is predominantly produced through the process $e^+e^- \to D_s^{*+}D_s^-$, where the D_s^{*+} decays to either γD_s^+ or $\pi^0 D_s^+$. As a consequence, any event that contains a D_s^+ meson also contains a D_s^- meson. This condition enables the usage of a powerful "double tag (DT)" technique [9] to measure absolute BFs. Events with at least one D_s^- tag candidate reconstructed, which are referred to as "single tag (ST)" events, provide a sample with a known number of $D_s^+D_s^-$ pairs. The ST events are selected by reconstructing a D_s^- meson in the two golden decays $D_s^- \to K_S^0K^-$ and $K^+K^-\pi^-$. The absolute BF of the signal mode ($\mathcal{B}_{\rm sig}$) is determined by forming D_s^+ signal candidates with $\omega\pi^+$ or ωK^+ from the tracks and clusters which are not used in the tag reconstruction in the events, where ω is reconstructed in the decay $\omega \to \pi^+\pi^-\pi^0$. The value of the BF is then obtained by

$$\mathcal{B}_{\rm sig} = Y_{\rm sig} \Big/ \sum_i \frac{Y^i_{\rm tag}\epsilon^i_{\rm tag,sig}}{\epsilon^i_{\rm tag}}, \qquad (1)$$

where $Y_{\rm sig}$ is DT yield, $\epsilon^i_{\rm tag,sig}$ is DT efficiency, and $Y^i_{\rm tag}$ and $\epsilon^i_{\rm tag}$ are ST yield and ST efficiency of the ith tag mode, respectively.

Simulations of the BESIII detector can be found in Ref. [10]. Two endcap time-of-flight systems were later upgraded with multigap resistive plate chambers [11]. Simulations of BESIII detector are based on GEANT4 [12]. A Monte Carlo (MC) sample, called "generic MC," includes all known open-charm processes, $e^+e^- \to \gamma J/\psi$ and $\gamma\psi(3686)$ due to the initial state radiation, and the processes without charm quark involved (continuum). The open-charm processes [8] are generated with CONEXC [13], considering the effects from initial state radiation and final state radiation. Decay modes with known BFs are simulated with EVTGEN [14]. The generators KKMC [15] and BABAYAGA [16] are used to simulate the continuum. The generic MC, corresponding to an effective luminosity of 110.6 fb^{-1}, is used to determine the ST efficiency and estimate the background. An MC sample of $D_s^+ \to \omega\pi^+$ or $D_s^+ \to \omega K^+$, along with D_s^- decaying to any known final states is generated to estimate the DT efficiency, which is called "signal MC."

The tag and signal candidates are constructed from individual π^+, K^+, K_S^0 and π^0 candidates in an event, where K_S^0 and π^0 are reconstructed from the decays $K_S^0 \to \pi^+\pi^-$ and $\pi^0 \to \gamma\gamma$, respectively. All charged tracks, except K_S^0 daughters, are required to originate from within 10 cm (1 cm) along (perpendicular to) beam axis with respect to interaction point (IP) of the e^+e^- beams. The track polar angle (θ) is required to be within $|\cos\theta| < 0.93$. The combination of information about energy loss in multilayer drift chamber and time-of-flight is used to identify the species of charged particles by calculating a confidence level CL_K or CL_π that the track satisfies the hypothesis of being a K or π. The charged K and π candidates are required to satisfy $CL_K > CL_\pi$ and $CL_\pi > CL_K$, respectively. The momenta of all pions are required to be greater than 0.1 GeV/c, in order to reject low momentum pions produced in D^* decay.

For K_S^0 candidates, the related combinations of two oppositely charged tracks with mass hypotheses being set to m_π [8] are required to have an invariant mass in the interval $[0.487, 0.511]$ GeV/c^2. Here, the particle identification (PID) is not applied and the distances of closest approach to the IP are required to be less than 20 cm along the beam axis.

The energy of each photon from the π^0 decay is required to be larger than 25 (50) MeV in the barrel (endcap) region of the electromagnetic calorimeter [10]. The opening angles between the photon and all the charged tracks should be larger than 10°. The invariant mass of the $\gamma\gamma$ pair is required to be within the asymmetric intervals $[0.115, 0.150]$ GeV/c^2. Furthermore, the π^0 candidates are constrained to their nominal mass [8] via a kinematic fit to improve their energy and momentum resolution.

For D_s candidate, the recoil mass $M_{\rm rec}$ is evaluated, $M_{\rm rec} = \sqrt{(E_{\rm tot} - \sqrt{p^2_{D_s} + m^2_{D_s}})^2 - |\vec{p}_{\rm tot} - \vec{p}_{D_s}|^2}$, where $E_{\rm tot}$, p_{D_s}, m_{D_s}, $\vec{p}_{\rm tot}$ and $\vec{p}_{D_s}$ are the total energy of e^+e^-, the momentum of the D_s candidate, the nominal mass of D_s [8], the three-momentum vector of the colliding e^+e^- system, and the three-momentum vector of the

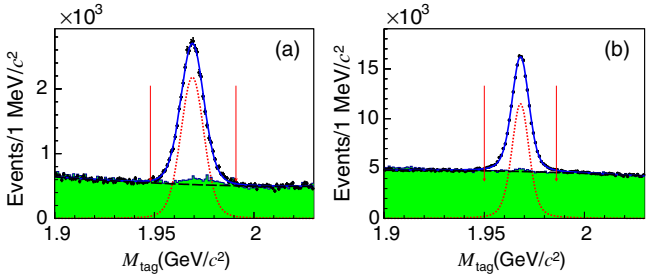

FIG. 1. Fits to the $M_{\rm tag}$ spectra of (a) $D_s^+ \to K_S^0 K^+$ and (b) $D_s^+ \to K^- K^+ \pi^+$. The dots with error bars are data, the solid lines are the total fits, the dashed lines and the dotted lines are the shapes of signal and fitted background, respectively. The (green) filled histograms are the MC-simulated backgrounds. The D_s signal regions are between the arrows.

reconstructed D_s candidate, respectively. To select the $D_s^* D_s$ sample, the invariant mass and $M_{\rm rec}$ of all candidates are required to fall into the ranges $[1.90, 2.03]$ GeV/c^2 and $[2.05, 2.18]$ GeV/c^2, respectively. If there are multiple tag candidates for each mode in an event, the one with $M_{\rm rec}$ closest to $m_{D_s^*}$ [8] is chosen.

The ST yield in each decay is extracted from a fit to the invariant mass spectrum ($M_{\rm tag}$) of the ST D_s^- candidates. The fit results are shown in Fig. 1. The signal shape is modeled as a double Gaussian function (the sum of two Gaussian functions whose area ratio is left free), while the background is parametrized as a second-order Chebychev polynomial. Signal regions are defined as $[1.948, 1.991]$ GeV/c^2 for $D_s^- \to K_S^0 K^-$ and $[1.950, 1.986]$ GeV/c^2 for $D_s^- \to K^+ K^- \pi^-$, respectively. The ST yields in the signal regions determined by the fit for $D_s^- \to K_S^0 K^-$ and $D_s^- \to K^+ K^- \pi^-$ are 32751 ± 310 and 131862 ± 770, respectively. For the tag mode $D_s^- \to K_S^0 K^-$, a small peak of background events is observed in the signal region; this is due to $D^- \to K_S^0 \pi^-$ events with the π^- misidentified as a K^-. From the generic MC, the $D^- \to K_S^0 \pi^-$ background is estimated to be around 250 events, corresponding to about 0.2% of the total ST yields, which is considered in the systematic uncertainty. For the tag mode $D_s^- \to K^+ K^- \pi^-$, a much smaller bump can also be found and the effect is negligible. For ST events with D_s^+ signal candidates, we require that at least one of two candidates have $M_{\rm rec}$ greater than 2.10 GeV/c^2. If there is more than one signal candidate for each mode, the one with an average invariant mass of the two D_s mesons closest to m_{D_s} is chosen.

Since the signal events are expected to peak at the ω mass in $\pi^+\pi^-\pi^0$ invariant mass ($M_{\pi^+\pi^-\pi^0}$) spectrum, $M_{\pi^+\pi^-\pi^0}$ is required to be within the interval $[0.60, 0.95]$ GeV/c^2. For $D_s^+ \to \omega\pi^+$, two $\pi^+\pi^-\pi^0$ combinations are formed in each event. In the data sample, there are 5 events with both $\pi^+\pi^-\pi^0$ combinations retained, which correspond to about 1% of all selected events. According to studies of generic MC, these events do not form any peak, thus they are neglected. For $D_s^+ \to \omega K^+$, background from the decay $D_s^+ \to K_S^0 K^+ \pi^0$ has the same final-state particles as signal and forms a peak around the $K^*(892)$ mass in the $M_{\pi^+\pi^-\pi^0}$ spectrum. We further perform a K_S^0 veto to suppress this background. If the invariant mass of the $\pi^+\pi^-$ ($M_{\pi\pi}$) combination in a $D_s^+ \to \omega K^+$ signal candidate satisfies $|M_{\pi\pi} - m_{K_S^0}| < 0.03$ GeV/c^2 and the distance between the decay point and the IP has a significance of more than two standard deviations, the candidate is vetoed. This veto eliminates about 78% of $D_s^+ \to K_S^0 K^+ \pi^0$ background, while retaining about 97% of signal events. After the K_S^0 veto, this background is found to be negligible according to the generic MC.

TABLE I. The ST efficiencies $\epsilon_{\rm tag}$ and DT efficiencies $\epsilon_{\rm tag,sig}$.

Tag mode	$\epsilon_{\rm tag}$ (%)	$\epsilon_{{\rm tag},\omega\pi^+}$ (%)	$\epsilon_{{\rm tag},\omega K^+}$ (%)
$D_s^- \to K_S^0(\pi^+\pi^-)K^-$	51.38 ± 0.25	12.53 ± 0.13	10.74 ± 0.11
$D_s^- \to K^+K^-\pi^-$	38.44 ± 0.08	979 ± 0.06	8.81 ± 0.06

The ST and DT efficiencies are determined from the generic MC and signal MC samples, respectively. All efficiencies are summarized in Table I.

The scatter plots of signal invariant mass spectrum ($M_{\rm sig}$) vs $M_{\pi^+\pi^-\pi^0}$ for the two signal decays are shown in Fig. 2. The correlation between $M_{\rm sig}$ and $M_{\pi^+\pi^-\pi^0}$ for events away from the signal peak between $M_{\rm sig}$ and $M_{\pi^+\pi^-\pi^0}$ is found to be -0.12 (0.39) for $D_s^+ \to \omega\pi^+(K^+)$. The signal events are expected to peak at the D_s mass in the $M_{\rm sig}$ distribution and at the ω mass in the $M_{\pi^+\pi^-\pi^0}$ distribution. Thus we employ a two-dimensional (2D) fit to $M_{\rm sig}$ vs $M_{\pi^+\pi^-\pi^0}$ distribution. Here, we neglect the correlation effect and consider it as a systematic uncertainty due to the fit procedure and correlations. The fit function is the sum of signal and background contributions, which are the products of corresponding one-dimensional (1D) functions described in the next paragraph. The signal function is the product of D_s signal function and ω signal function. The background is the sum of three contributions: background neither peaking in the $M_{\pi^+\pi^-\pi^0}$ distribution nor the $M_{\rm sig}$ distribution (BKGI), background peaking around the ω mass in the $M_{\pi^+\pi^-\pi^0}$ distribution (BKGII), and background peaking around the D_s mass in the $M_{\rm sig}$ distribution (BKGIII).

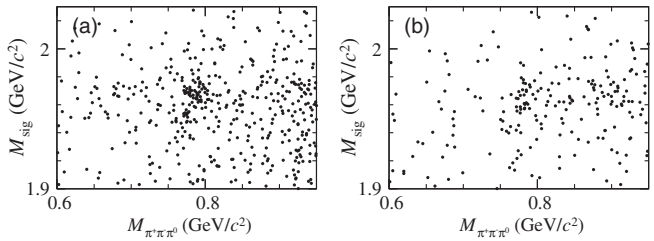

FIG. 2. The scatter plots of $M_{\rm sig}$ vs $M_{\pi^+\pi^-\pi^0}$ for (a) $D_s^+ \to \omega\pi^+$ and (b) $D_s^+ \to \omega K^+$.

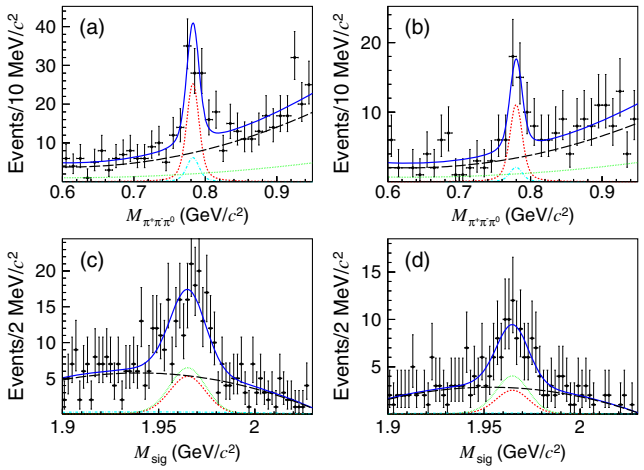

FIG. 3. The projections of [(a) and (b)] $M_{\pi^+\pi^-\pi^0}$, and for [(c) and (d)] $M_{\rm sig}$ for the results of (a,c) $D_s^+ \to \omega\pi^+$ and (b, d) $D_s^+ \to \omega K^+$. The dots with error bars are data, the (blue) solid lines describe the total fits, the (red) dashed lines describe the signal and the (dark green) dotted, (violet) dash-dotted, and (black) long dashed lines describe the BKGI, BKGII, and BKGIII, respectively. The BKGII comes from the non-D_s processes involving ω. The BKGIII comes from the contributions of other D_s^+ decays to $\pi^+\pi^-\pi^0\pi^+$ and $\pi^+\pi^-\pi^0K^+$ final states for $D_s^+ \to \omega\pi^+$ and $D_s^+ \to \omega K^+$, respectively.

The BKGI is modeled as the product of D_s background function and ω background function. The BKGII (BKGIII) is modeled as the product of the D_s background (signal) function and ω signal (background) function.

The D_s signal function is constructed as the MC-simulated shape convolved with a Gaussian function. This Gaussian function describes the resolution difference between data and MC simulation. The D_s background function is a second-order Chebychev polynomial. The parameters in D_s signal function and D_s background function are determined in the fit to $M_{\rm sig}$ spectrum of data. The ω signal function is constructed as a Breit-Wigner function convolved with a Gaussian function. This convolved Gaussian function describes the detector resolution and its width is fixed to the value determined from a sample of $e^+e^- \to K^+K^-\omega$, whose observed yield is greater than the signal by two orders of magnitude. The ω background function is described with a second-order Chebychev polynomial. All parameters in ω signal function and ω background function are determined by the fit to $M_{\pi^+\pi^-\pi^0}$ spectrum of data, except for the width of Gaussian function in ω signal function.

From the 2D fits, shown in Fig. 3, we obtain 65.0 ± 11.6 $D_s^+ \to \omega\pi^+$ signal events and 28.5 ± 7.8 $D_s^+ \to \omega K^+$ signal events with statistical significances of 6.7σ and 4.4σ, respectively. With Eq. (1) and the world averaged BFs of $\omega \to \pi^+\pi^-\pi^0$ and $\pi^0 \to \gamma\gamma$ [8], the BFs are measured to be: $\mathcal{B}(D_s^+ \to \omega\pi^+) = (1.77 \pm 0.32) \times 10^{-3}$ and $\mathcal{B}(D_s^+ \to \omega K^+) = (0.87 \pm 0.24) \times 10^{-3}$, where the uncertainties are statistical. The systematic uncertainties are estimated and summarized in Table II, where the total systematic uncertainty is obtained by adding the individual terms in quadrature.

TABLE II. Relative systematic uncertainties (%) in the BF measurements.

Source	$D_s^+ \to \omega\pi^+$	$D_s^+ \to \omega K^+$
$M_{\rm rec}$ requirement	0.1	
Momentum requirement on pion	1.7	
K_S^0 veto	...	0.1
PID of $K^\pm$,$\pi^\pm$	1.5	1.5
Tracking of $K^\pm$,$\pi^\pm$	3.0	3.0
π^0 reconstruction	1.8	1.9
MC statistics	0.6	0.6
Background description	4.1	4.6
Signal description	3.3	5.3
ST yield determination	1.3	1.3
Fit procedure and correlation	2.4	
$\mathcal{B}(\omega \to \pi^+\pi^-\pi^0)$ & $\mathcal{B}(\pi^0 \to \gamma\gamma)$	0.8	
Total	7.4	8.7

All the systematic uncertainties due to the selection criteria come from the differences of the selection efficiencies between data and MC simulation. The uncertainties due to the $M_{\rm rec}$ requirement and pion-momentum requirement are 0.1% and 1.7%, respectively. They are estimated with a control sample of $D_s^+ \to \pi^+\pi^-\pi^+\eta$, $\eta \to \gamma\gamma$, with η' decays removed by requiring the invariant mass of $\pi^+\pi^-\eta$ to be greater than $1.0\,{\rm GeV}/c^2$, where the selection criteria of η are the same as those used for π^0 expect that the $\gamma\gamma$ invariant mass window is $[0.490, 0.580]\ {\rm GeV}/c^2$. The uncertainty due to the K_S^0 veto is 0.1%, which is estimated with a control sample of $D^0 \to K_S^0\omega$. The uncertainties for charged tracks selection are determined to be 0.5%/track for PID and 1.0%/track for tracking using a control sample of $e^+e^- \to K^+K^-\pi^+\pi^-$. The uncertainty of the π^0 reconstruction efficiency is estimated with a control sample of $e^+e^- \to K^+K^-\pi^+\pi^-\pi^0$, and is determined to be 1.8% (1.9%) for $D_s^+ \to \omega\pi^+(K^+)$. The uncertainty due to the MC statistics is 0.6%.

The uncertainties due to the background description are 4.1% and 4.6% for $D_s \to \omega\pi^+$ and $D_s \to \omega K^+$, respectively. They are estimated by narrowing the fit ranges of $M_{\pi^+\pi^-\pi^0}$ and $M_{\rm sig}$ to $[0.65, 0.90]\ {\rm GeV}/c^2$ and $[1.91, 2.02]\ {\rm GeV}/c^2$, respectively, and replacing the second-order Chebychev polynomial in $f_{D_s}^{\rm poly}$ and $f_\omega^{\rm poly}$ by a first-order Chebychev polynomial. The uncertainties due to the signal description are 3.3% and 5.3% for $D_s \to \omega\pi^+$ and $D_s \to \omega K^+$, respectively. They are estimated by varying the masses and resolutions of the ω and D_s within their uncertainties [17]. The uncertainty related to ST yield determination is 1.3%, including the effects from signal shape, background shape and fit range in the fits

to $M_{\rm tag}$ spectra. The effect from signal shape is estimated by replacing the MC-simulated shape with the Gaussian function, where the effect from the bump under the $D_s^- \to K_S^0 K^-$ signal region is also taken into account. The effects from background shape and fit ranges, which are estimated with the same method as the assignment for D_s background shape, are found to be negligible. The uncertainty due to the fit procedure and correlation is estimated by studying thirty statistically independent samples of generic MC events with the same size as data. With the same method as used in the data analysis, the average measured BF is found to have a relative difference of 0.8% with respect to the input value. Conservatively, an uncertainty of 2.3% from MC statistic is also included, thus the uncertainty in the fit procedure and correlation is 2.4%. The uncertainty related to the assumed BFs for $\omega \to \pi^+\pi^-\pi^0$ and $\pi^0 \to \gamma\gamma$ is 0.8%, which is taken from the PDG [8].

In summary, we observe the W-annihilation decay $D_s^+ \to \omega\pi^+$ with a significance of 6.7σ and measure its BF to be $(1.77 \pm 0.32_{\rm stat} \pm 0.13_{\rm sys}) \times 10^{-3}$. This measurement provides critical information to determine the nonperturbative W-annihilation amplitudes, benefits the investigations of the underlying dynamics in charmed hadronic decays, and will allow better predictions for the BFs and direct CPV of decays involving W-annihilation [1,3–5]. Among these decays, $D_s^+ \to \omega K^+$ is of interest for its possibly large CPV. We find the first evidence for this decay with a significance of 4.4σ. Its BF is measured to be $(0.87 \pm 0.24_{\rm stat} \pm 0.08_{\rm sys}) \times 10^{-3}$. According to Ref. [3], our result implies that direct CP asymmetry in this decay is expected to be -0.6×10^{-3}. Considering the CP asymmetry in D decays is at most at the level of 10^{-3} [8], we conclude that $D_s^+ \to \omega K^+$ is a good decay to search for CP violation.

ACKNOWLEDGMENTS

The authors wish to thank Fusheng Yu for useful discussions. The BESIII collaboration thanks the staff of BEPCII and the IHEP computing center for their strong support. This work is supported in part by National Key Basic Research Program of China under Contract No. 2015CB856700; National Natural Science Foundation of China (NSFC) under Contracts No. 11425524, No. 11625523, and No. 11635010; the Chinese Academy of Sciences (CAS) Large-Scale Scientific Facility Program; the CAS Center for Excellence in Particle Physics (CCEPP); Joint Large-Scale Scientific Facility Funds of the NSFC and CAS under Contracts No. U1332201, No. U1532257, and No. U1532258; CAS Key Research Program of Frontier Sciences under Contracts No. QYZDJ-SSW-SLH003 and No. QYZDJ-SSW-SLH040; 100 Talents Program of CAS; National 1000 Talents Program of China; INPAC and Shanghai Key Laboratory for Particle Physics and Cosmology; German Research Foundation DFG under Contracts No. Collaborative Research Center CRC 1044, FOR 2359; Istituto Nazionale di Fisica Nucleare, Italy; Koninklijke Nederlandse Akademie van Wetenschappen (KNAW) under Contract No. 530-4CDP03; Ministry of Development of Turkey under Contract No. DPT2006K-120470; National Science and Technology fund; The Swedish Research Council; U.S. Department of Energy under Contracts No. DE-FG02-05ER41374, No. DE-SC-0010118, No. DE-SC-0010504, and No. DE-SC-0012069; University of Groningen (RuG) and the Helmholtzzentrum fuer Schwerionenforschung GmbH (GSI), Darmstadt; WCU Program of National Research Foundation of Korea under Contract No. R32-2008-000-10155-0.

[1] H. Y. Cheng and C. W. Chiang, Phys. Rev. D **85**, 034036 (2012); **85**, 079903(E) (2012).
[2] H. N. Li, C. D. Lü, and F. S. Yu, Phys. Rev. D **86**, 036012 (2012).
[3] Q. Qin, H. N. Li, C. D. Lü, and F. S. Yu, Phys. Rev. D **89**, 054006 (2014).
[4] H. Y. Cheng and C. W. Chiang, Phys. Rev. D **81**, 074021 (2010).
[5] H. Y. Cheng, C. W. Chiang, and A. L. Kuo, Phys. Rev. D **93**, 114010 (2016).
[6] R. Balest *et al.* (CLEO Collaboration), Phys. Rev. Lett. **79**, 1436 (1997).
[7] J. Y. Ge *et al.* (CLEO Collaboration), Phys. Rev. D **80**, 051102(R) (2009).
[8] M. Tanabashi *et al.* (Particle Data Group), Phys. Rev. D **98**, 030001 (2018).
[9] R. M. Baltrusaitis *et al.* (Mark III Collaboration), Phys. Rev. Lett. **56**, 2140 (1986).
[10] M. Ablikim *et al.* (BESIII Collaboration), Nucl. Instrum. Methods Phys. Res., Sect. A **614**, 345 (2010).
[11] X. Wang *et al.*, J. Instrum. **11**, C08009 (2016).
[12] S. Agostinelli *et al.* (GEANT4 Collaboration), Nucl. Instrum. Methods Phys. Res., Sect. A **506**, 250 (2003).
[13] R. G. Ping, Chin. Phys. C **38**, 083001 (2014).
[14] D. J. Lange, Nucl. Instrum. Methods Phys. Res., Sect. A **462**, 152 (2001); R. G. Ping, Chin. Phys. C **32**, 599 (2008).
[15] S. Jadach, B. F. L. Ward, and Z. Was, Phys. Rev. D **63**, 113009 (2001).
[16] C. M. Carloni Calame, G. Montagna, O. Nicrosini, and F. Piccinini, Nucl. Phys. B, Proc. Suppl. **131**, 48 (2004).
[17] Throughout this paper, for resolutions determined by 1D fits and control samples, the given uncertainties are used to estimate the systematic uncertainties due to signal description. For the masses and widthes of particles, which fixed at PDG values. The uncertainties from PDG are used to estimate the systematic uncertainties due to signal description.